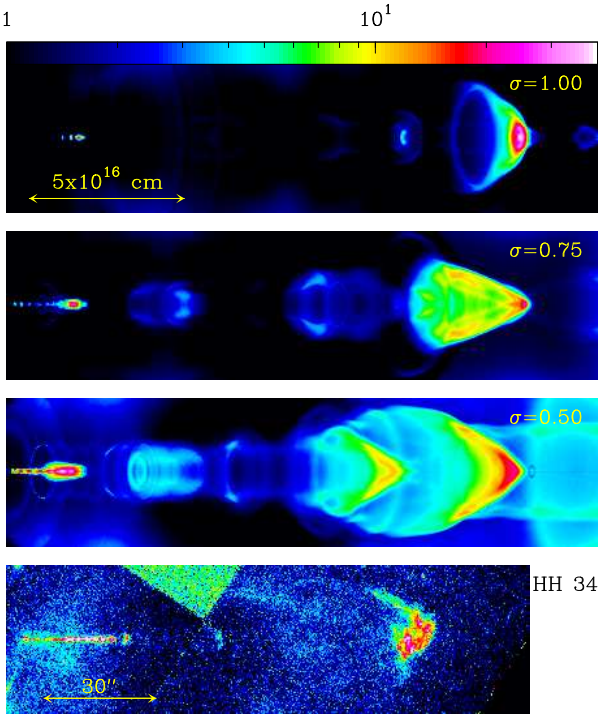

Fig. 4. [S II] 6716+30 intensity maps predicted from the three 3-mode jet models for a time $t = 0$ (the integration was started at $t = -3000$ yr, see § 4). The bottom frame shows the [S II] image obtained with the HST in 1998 (see § 2). The predicted maps have been computed assuming that the outflow axis lies at a 30° angle with respect to the plane of the sky (as appropriate for HH 34), and show a $(10.69, 2.67) \times 10^{17}$ cm domain. The HH 34 [S II] map has been scaled to the same scale as the predicted maps, assuming a distance of 450 pc (the displayed region has a vertical size of 39″.6). The source of HH 34 is on the left of the chain of aligned knots. The intensities are shown with a logarithmic color scheme covering a dynamic range of 40 (see the top bar), scaled so that in the four maps the brighter regions start to saturate at the highest depicted intensity. The color figure can be viewed online.

In Figure 4, we present the [S II] 6716+30 intensity maps predicted from these three models for $t = 0$ (i.e., for years ∼1990–1994 at which the data analyzed by Raga et al. 2002 were obtained). These maps were computed assuming a 30° angle between the jet axis and the plane of the sky, corresponding to the approximate orientation of the HH 34 outflow (see Heathcote & Reipurth 1992). Together with the predicted maps, we show an archival [S II] HST image of the southern lobe of the HH 34 outflow, rotated so that the outflow axis is parallel to the abscissa. The physical size of the domains of the synthetic and observed maps are identical (assuming a 450 pc distance to HH 34).

For all of the computed models, emission structures with a qualitative resemblance to HH 34 are obtained. The four models show a large bow shock at a distance from the source comparable to HH 34S, a chain of knots close to the source, and a few broader, faint condensations between the chain of knots and the large bow shock. These three main features are in qualitative agreement with the observed structure of the HH 34 jet.

It is clear from Figure 4 that the shape of the large bow shock is more flat-topped in the $\sigma = 1$ model than in the $\sigma = 0.75$ and 0.5 models, in which the bow shock has a more conical morphology. Also, in the $\sigma = 1$ model (presented previously by Raga et al. 2002), the [S II] emission from the chain of knots is fainter than the emission from the large bow shock. The $\sigma = 0.75$ and 0.5 models show a comparable peak [S II] emission in the main bow shock and in the brighter knots in the chain, in better qualitative agreement with the [S II] image of HH 34.

Figures 5, 6 and 7 show the time-evolution of the [S II] emission of the chain of knots for the $\sigma = 1$, 0.75 and 0.5 models (respectively), at 100 yr intervals. In the 300 yr time-sequence obtained from the $\sigma = 1$ model (Figure 5), we see either one or two groups of compact knots. The predicted emission is qualitatively different from the emission from the HH 34 jet (bottom panel), in which the inter-knot regions show considerably brighter emission. Also, some of the observed knots have bow shapes which are not seen in the maps predicted from the $\sigma = 1$ model.

The time-sequence of [S II] intensity maps obtained from the $\sigma = 0.75$ model (Figure 6) does show bow-shaped knots. The inter-knot regions show brighter emission, in better qualitative agreement with the HH 34 jet observation.

The emission maps obtained from the $\sigma = 0.5$ model show groups of knots having less contrast between the knot and inter-knot emission than the HH 34 jet. Because of this, we conclude that the $\sigma = 0.75$ model produces the best qualitative agreement with the structure of knots along the HH 34 jet. In the following, we therefore focus on the $\sigma = 0.75$ model.

In Figures 8 and 9 we show a sequence of intensity maps with a time-interval of 10 yr, together with the 1998 and 2007 HST [S II] images (see § 2). From these figures, it is clear that the knots along the HH 34 jets have changed quite strongly over a